DNA Origami Substrates for Highly Sensitive Surface-Enhanced Raman Scattering

ARTICLE *in* JOURNAL OF PHYSICAL CHEMISTRY LETTERS · DECEMBER 2013

Impact Factor: 7.46 · DOI: 10.1021/jz402076b

7 AUTHORS, INCLUDING:

Julia Prinz
Universität Potsdam
2 PUBLICATIONS **12** CITATIONS
SEE PROFILE

Lydia Olejko
Universität Potsdam
4 PUBLICATIONS **16** CITATIONS
SEE PROFILE

Jana Oertel
Helmholtz-Zentrum Dresden-Rossendorf
7 PUBLICATIONS **82** CITATIONS
SEE PROFILE

Ilko Bald
Universität Potsdam
49 PUBLICATIONS **718** CITATIONS
SEE PROFILE

THE JOURNAL OF PHYSICAL CHEMISTRY Letters

Letter

pubs.acs.org/JPCL

DNA Origami Substrates for Highly Sensitive Surface-Enhanced Raman Scattering

Julia Prinz,[‡] Benjamin Schreiber,[†,#] Lydia Olejko,[‡] Jana Oertel,[⊥] Jenny Rackwitz,[‡] Adrian Keller,*[,†] and Ilko Bald*[,‡,§]

[‡]Institute of Chemistry − Physical Chemistry, University of Potsdam, Potsdam, Germany

[†]Institute of Ion Beam Physics and Materials Research and [⊥]Institute of Resource Ecology, Helmholtz-Zentrum Dresden-Rossendorf, Dresden, Germany

[#]Technische Universität Dresden, Dresden, Germany

[§]BAM Federal Institute of Materials Research and Testing, Berlin, Germany

Supporting Information

ABSTRACT: DNA nanotechnology holds great promise for the fabrication of novel plasmonic nanostructures and the potential to carry out single-molecule measurements using optical spectroscopy. Here, we demonstrate for the first time that DNA origami nanostructures can be exploited as substrates for surface-enhanced Raman scattering (SERS). Gold nanoparticles (AuNPs) have been arranged into dimers to create intense Raman scattering hot spots in the interparticle gaps. AuNPs (15 nm) covered with TAMRA-modified DNA have been placed at a nominal distance of 25 nm to demonstrate the formation of Raman hot spots. To control the plasmonic coupling between the nanoparticles and thus the field enhancement in the hot spot, the size of AuNPs has been varied from 5 to 28 nm by electroless Au deposition. By the precise positioning of a specific number of TAMRA molecules in these hot spots, SERS with the highest sensitivity down to the few-molecule level is obtained.

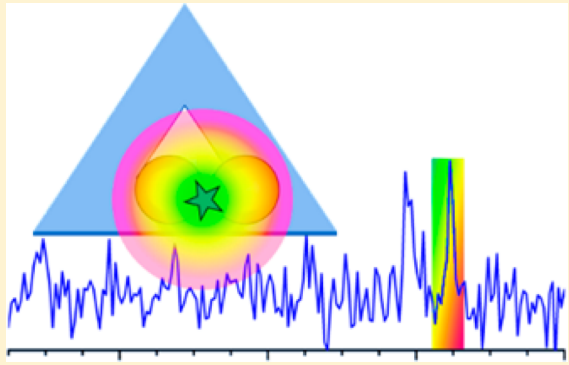

SECTION: Physical Processes in Nanomaterials and Nanostructures

Surface-enhanced Raman scattering (SERS)[1] provides both single-molecule sensitivity[2−5] and rich chemical information and thus enables the multiplexed detection of analyte molecules at trace levels.[6] DNA-based plasmonic nanostructures such as nanogap particles and nanodumbbells were shown to be very efficient SERS substrates with extremely high enhancement factors for Raman scattering.[7−9] However, a versatile SERS substrate requires not only a controlled arrangement of nanoparticles but also specific anchor points for analyte molecules to enable quantitative analyte detection. The fabrication of substrates for highly sensitive and quantitative SERS represents the greatest challenge in current SERS research as it requires (i) a precise arrangement of metal nanoparticles to optimize the Raman scattering from the SERS hot spot, (ii) sophisticated surface functionalization for the immobilization of analytes in the hot spot, and (iii) accurate control of analyte concentration in the SERS hot spots. In this work, we thus demonstrate SERS from gold nanoparticle (AuNP) dimers immobilized on DNA origami substrates with a specific number of analyte molecules positioned in the hot spots in between the AuNPs.

DNA origami nanostructures[10] are versatile substrates for arranging metal nanoparticles into two- and three-dimensional arrays.[11−13] Due to the tunable plasmonic coupling between the nanoparticles, assemblies with tailored optical properties can be synthesized in this way.[13] DNA origami nanostructures furthermore enable the spatially controlled positioning of single analyte molecules with nanometer precision, which has recently been exploited in fluorescence enhancement studies.[14,15] The use of DNA origami nanostructures as scaffolds to arrange AuNPs thus allows for the engineering of SERS hot spots by control of the interparticle gap and precise quantification and positioning of molecules in these gaps.

The DNA−AuNP hybrids presented here are based on triangular DNA origami nanostructures, which are formed by hybridization of the single-stranded (ss) M13mp18 viral DNA scaffold with a suitable set of 208 short staple strands.[10] Selected staple strands can be individually modified for instance for the binding of analyte molecules, or they can be simply extended to provide protruding ss anchoring sites for the hybridization with DNA-coated AuNPs. To bind the AuNPs, three adjacent staple strands for each AuNP are extended with a capture sequence (see the Experimental Methods section for details). The AuNPs are coated with thiol-modified ssDNA,

Received: September 26, 2013
Accepted: November 19, 2013
Published: November 19, 2013

   dx.doi.org/10.1021/jz402076b | J. Phys. Chem. Lett. 2013, 4, 4140−4145

complementary to the capture sequences located on the DNA origami structure (Figure 1).[12] By hybridization, two AuNPs

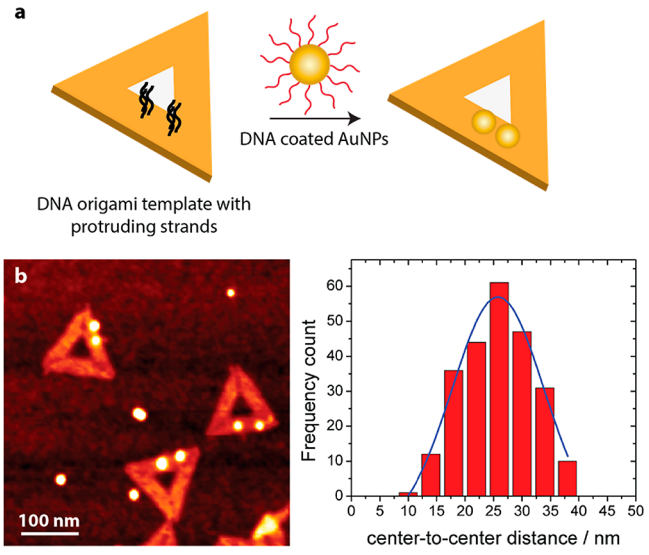

Figure 1. Immobilization of AuNPs on DNA origami triangles. (a) Scheme illustrating the attachment of two DNA-coated AuNPs to the DNA origami substrate by DNA hybridization. (b) Atomic force microscopy (AFM) image of triangular DNA origami structures carrying two 5 nm AuNPs at a nominal distance of 25 nm. The histogram shows the experimentally determined distribution of the center-to-center distance between the two AuNPs, which is based on AFM images (see the Supporting Information). The bin size was 4 nm.

are bound at predefined positions to one DNA origami triangle to form a dimer. Due to the coupling of the surface plasmon resonances of the individual AuNPs, a Raman hot spot is formed in the interparticle gap. Figure 1 shows triangular DNA origami structures with two 5 nm AuNPs placed at a nominal distance of 25 nm. The interparticle distance of a total of 242 individual AuNP–DNA origami assemblies was measured by AFM (see Supporting Information Figure S1 for a larger AFM image). In agreement with the nominal value, the resulting distribution in Figure 1b reveals an average interparticle distance of 25.8 nm with a fwhm of 18.9 nm.

To demonstrate the SERS detection of specific target molecules by means of the hybrid AuNP–DNA origami structures, we used carboxytetramethylrhodamine (TAMRA) as a Raman reporter molecule. In initial experiments, we coated 15 nm AuNPs with thiol-modified ssDNA, carrying a TAMRA modification at the 5′-side of the thiol group (Figure 2a). Figure 2b shows an AFM image of disperse DNA/TAMRA-modified AuNPs adsorbed to an oxidized Si wafer. The corresponding SERS spectrum shown in Figure 2d was collected by confocal Raman microscopy using a 532 nm laser for Raman excitation. Previous studies revealed only a rather weak electric field enhancement in the vicinity of single AuNPs upon excitation of the surface plasmon resonance, resulting in an enhancement factor of $10-10^3$ depending on the size of the AuNPs.[16] Consequently, the blue SERS spectrum in Figure 2d shows only a very weak TAMRA-characteristic signal at around 1650 cm^{-1}. However, the Raman signal becomes considerably stronger when the AuNPs are bound to DNA origami nanostructures at a distance of 25 nm to form AuNP dimers (see the red spectrum in Figure 2d). An AFM image of

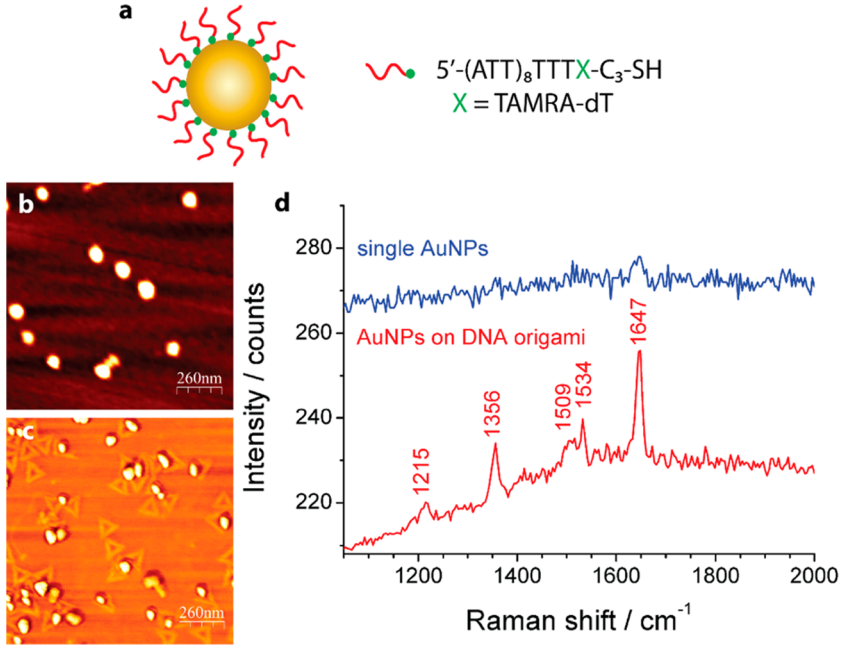

Figure 2. SERS measurements using TAMRA-coated AuNPs. (a) Illustration of AuNPs functionalized with DNA via a thiol group. The ssDNA is additionally modified with the fluorescent dye TAMRA (green) at the position indicated with X. (b,c) AFM images of 15 nm TAMRA–DNA-coated AuNPs (b) dispersed on a Si/SiO_2 substrate and (c) arranged on DNA origami substrates. (d) SERS spectra obtained from the samples shown in (b) and (c). For dispersed and isolated AuNPs, only a weak SERS signal is detected at around 1650 cm^{-1}. The SERS spectrum of the DNA origami-bound AuNPs on the other hand shows bands at 1647, 1534, 1509, 1356, and 1215 cm^{-1}, which correspond to the characteristic SERS signals of TAMRA. The comparatively strong SERS signal is due to the DNA origami-directed formation of hot spots between the two AuNPs. The blue spectrum is shifted vertically by 65 counts. On average, the concentration of AuNPs in the DNA origami samples (red spectrum) is about 2.6 times higher than that of the single AuNP sample (blue spectrum).

dx.doi.org/10.1021/jz402076b | J. Phys. Chem. Lett. 2013, 4, 4140–4145

TAMRA–AuNP–DNA origami substrates is shown in Figure 2c. The visible Raman bands at 1647, 1534, 1509, 1356, and 1215 cm^{-1} are all characteristic SERS bands for TAMRA.[17,18] Due to the close proximity of the AuNPs on the DNA origami substrates, the surface plasmon resonances of the individual AuNPs can couple to form localized hot spots with particularly high electric field enhancement, which results in a correspondingly strong Raman signal. To exclude a Raman enhancement due to image charges on Si,[19] different substrates have been used for DNA origami adsorption, and no differences were found in the SERS intensity (Figure S4, Supporting Information).

However, it is not clear how many TAMRA molecules are located in the hot spots and contribute to the SERS signal. The red Raman spectrum shown in Figure 2d originates mainly from the TAMRA molecules located within the hot spots between the two AuNPs. To estimate the total number of molecules contributing to the SERS signal, we consider the laser focus area of 1.3 μm^2. On the basis of our AFM images, we can assume that on average about 12 well-assembled DNA origami structures are located in the laser focus area and that each 15 nm AuNP is covered by a maximum of 200 oligonucleotides,[20] about 10% of which are actually located in the hot spots. Accordingly, the total number of molecules contributing to the signal is on the order of 10^2–10^3.

However, with the DNA origami technique, it is possible to exactly control the number of dye molecules in the hot spot. To this end, we modified three staple strands in the DNA origami substrate with TAMRA at the 5′-end such that the three TAMRA molecules were placed in between the AuNPs, that is, in the hot spot (Figure 3a). In this arrangement, the AuNPs were coated with DNA without TAMRA modification, that is, there are exactly three TAMRA molecules immobilized on each DNA origami triangle. Because the number of analyte molecules is considerably lower compared to the arrangement shown in Figure 2, the hot spots have to be further optimized in order to yield stronger electric field enhancement. When using 15 nm AuNPs at a distance of 25 nm, the gap size of 10 nm is too large to enable few-molecule detection. However, if larger AuNPs (e.g., 20 nm) are used, the yield of well-assembled AuNP dimers will be rather small due to steric hindrance. Therefore, we first immobilized two 5 nm AuNPs on the DNA origami substrates and increased their size by electroless Au deposition to optimize the gap size. By varying the incubation time, it was possible to exactly control the size of AuNPs on the DNA origami substrate and thus their interparticle gap (see Figure S5, Supporting Information). The diameters of the AuNPs have been extracted from their heights in AFM topography images, which were determined to be 12, 20, 25, and 28 nm. Subsequently, the samples have been analyzed by scanning electron microscopy (SEM) and Raman spectroscopy (Figure 3b). In addition to the SEM images and the SERS spectra obtained from the differently sized AuNPs, Figure 3b shows near-field simulations of the electric field enhancement in the vicinity of AuNPs in the discrete dipole approximation (DDA).[21,22] At a diameter of 20 nm, the surface plasmon resonances can couple, and a localized hot spot appears. The field enhancement is strongest at a diameter of 25 nm when the two AuNPs are almost in direct contact. At larger diameters, the two AuNPs are fused together and rather behave like rough nanorods, as indicated by the appearance of a strong second plasmon resonance in the absorbance spectra shown in Figure S6 (Supporting Information). This results in a weaker field

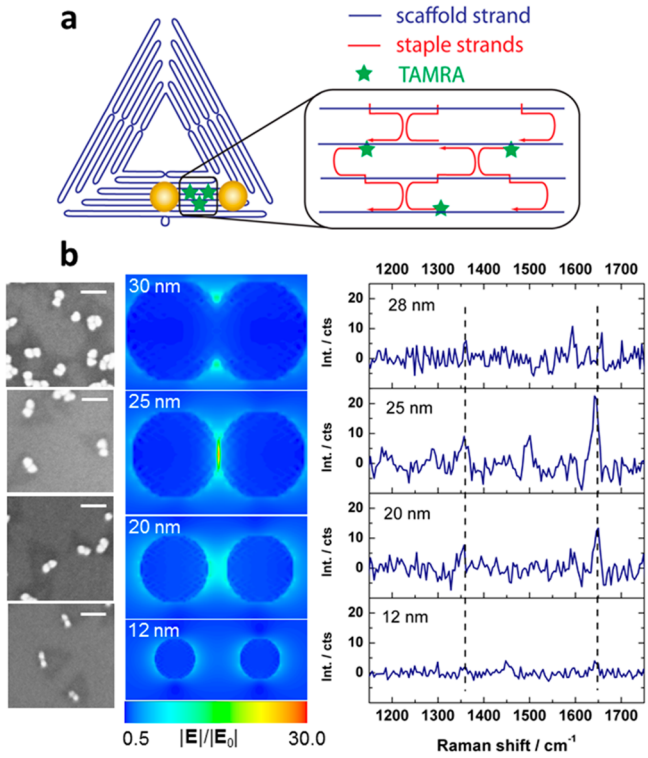

Figure 3. AuNPs arranged into dimers on DNA origami substrates with three single TAMRA molecules positioned in the resulting hot spots. (a) Scheme of the DNA origami substrate carrying three single TAMRA molecules between two AuNPs. In contrast to the system shown in Figure 2, no TAMRA is attached to the AuNPs. (b) Scanning electron micrographs of DNA origami–AuNP hybrid structures having AuNP diameters ranging from 12 to 28 nm (left, scale bar is 100 nm), the DDA simulations of the normalized electric field intensity $|\mathbf{E}|/|\mathbf{E}_0|$ in the vicinity of the AuNP dimers (center), and corresponding SERS spectra (right). The spectral positions indicated by the dashed lines are located at 1357 and 1647 cm^{-1}, respectively. The size of the AuNPs was controlled by electroless deposition of preattached 5 nm AuNPs. By variation of the deposition time, the size of the AuNPs can be precisely tuned. In the SERS spectra, the characteristic band of TAMRA at around 1650 cm^{-1} appears at a AuNP diameter of 20 nm, in agreement with the appearance of a localized hot spot in the DDA simulations. The intensity of both the hot spot and the corresponding SERS spectra reaches a maximum at a AuNP diameter of 25 nm. At about a 28 nm AuNP diameter, however, the TAMRA signal decreases considerably due to the fusing of the two AuNPs and consequently weaker and more localized hot spots, as is confirmed by the DDA simulations shown on the left.

enhancement localized around the ring in the center. The corresponding SERS spectra in Figure 3b confirm the results of the simulations (see also Figure S7 (Supporting Information) for comparison of the measured SERS intensity with the intensity of the electric field in the hot spot according to the simulations). The strongest bands in the SERS spectrum of TAMRA (located at around 1650 and 1350 cm^{-1}, the spectral positions are indicated by dashed vertical lines) are clearly visible for 20 nm particle size and become even more pronounced for 25 nm AuNPs. Additional signals result from the DNA surrounding the AuNPs. At larger AuNP diameter (28 nm), the TAMRA signal decreases considerably due to the weaker and more localized field enhancement when no gap between the AuNPs is present.

dx.doi.org/10.1021/jz402076b | J. Phys. Chem. Lett. 2013, 4, 4140–4145

These experiments demonstrate that detection of three TAMRA molecules per DNA origami structure is possible with SERS using optimized AuNP dimers. In order to explore the possibility of single-molecule detection, a single TAMRA molecule was placed in the hot spot of AuNPs with 25 nm diameter. The schematic of the SERS substrate, recorded SERS spectra, and an AFM image are shown in Figure 4. The red SERS spectrum is the same as that in Figure 2 (with the fluorescent background removed) and is shown as a reference. The black spectrum represents an average of several spots on the surface, whereas the blue spectrum was obtained from a single spot. Both spectra (black and blue) exhibit a weak band at 1647 cm^{-1} that corresponds to the most intense Raman band of TAMRA and thus originates from the single TAMRA molecules in the hot spots. The signal-to-noise ratio ($S/N = (I_{signal} - I_{baseline})/\sigma_{noise}$, with I being the signal intensity and σ the standard deviation) for this band is 5.8 (black spectrum) and 4.7 (blue spectrum), which is just above the detection limit of $S/N = 3$. Figure 4c shows an AFM image of the spot from which the blue SERS spectrum was recorded indicating that the Raman signal is due to a maximum of 17 DNA origami structures, that is, 17 independent single TAMRA molecules. The height profile shown in Figure 4c indicates that the AuNPs have an optimal diameter of 23−25 nm. This demonstrates the possibility to reach few-molecule sensitivity with optimized DNA origami-based SERS substrates. The additional Raman bands observed in the black spectrum in Figure 4b are due to the A/T-containing DNA sequences surrounding the AuNPs. The most pronounced DNA signal is detected at 1589 cm^{-1}, which is due to the C−N stretching vibration of the A ring.[23] The signal at 1275 cm^{-1} can also be assigned to the A ring, and the signal at 1093 cm^{-1} is due to the PO_2 stretching vibration within the DNA backbone.[24] The weak band at 1451 cm^{-1} can be assigned to third-order Raman scattering from the Si/SiO_2 substrate. Control experiments using AuNP dimers on DNA origami substrates without TAMRA modification did not show any signal at around 1650 cm^{-1} (Figure S8, Supporting Information).

In summary, we have demonstrated SERS from AuNP assemblies on DNA origami substrates. By exploiting the local addressability of the DNA origami nanostructures, AuNPs were arranged into dimers with tunable particle spacing in order to create localized and well-defined hot spots between the particles. We have shown that the electromagnetic field enhancement in the hot spots can be strong enough to excite specific and detectable Raman modes in fluorophores located in the hot spots. By optimizing the particle size and thus the gap size between the particles to obtain highest field enhancements, we were able to identify specific Raman bands of single TAMRA molecules attached to the DNA origami substrates.

Due to the high spatial control provided by the DNA origami technique, the hot spots can be further optimized, for instance, by realizing more complex nanoparticle arrays such as trimers of AuNPs.[25] Furthermore, our DNA origami-based SERS substrates can be developed into nanoscale SERS sensor chips by incorporating capture sites for target biomolecules into the hot spots. This can, for instance, be achieved by positioning a single aptamer in the hot spot that can bind to a single target protein.[26] Because the SERS technique provides rich chemical information, the combination of several target-specific DNA origami nanosensors may thus enable the multiplexed detection[6] of a variety of different analyte molecules at a single-molecule level.

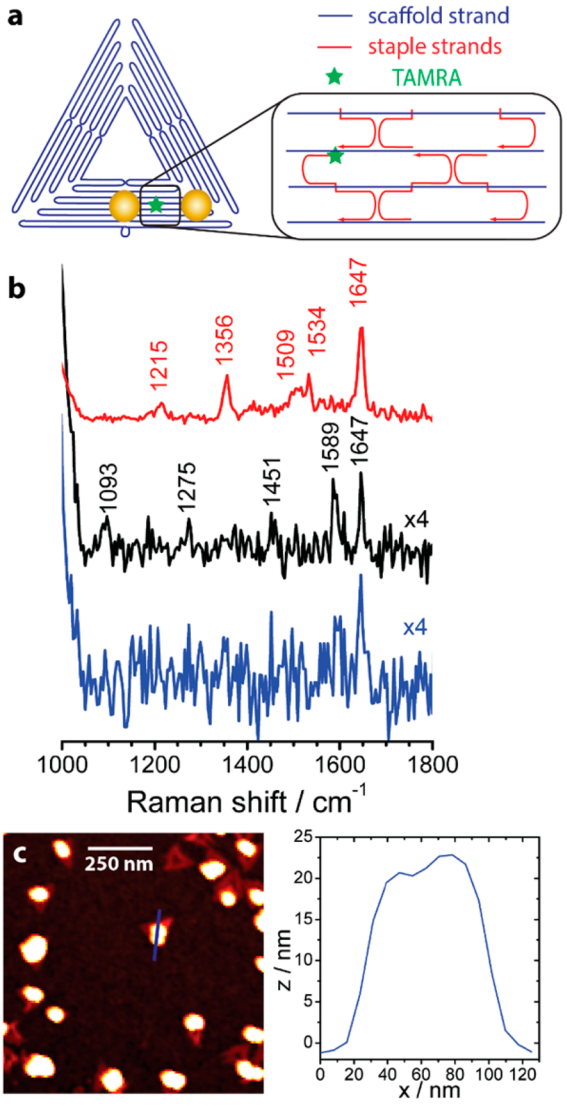

Figure 4. SERS measurements using DNA origami-directed AuNP dimers with a single TAMRA molecule placed in the hot spot. (a) Illustration showing the functionalization of the DNA origami substrate with a single TAMRA molecule in the center between two AuNPs. (b) SERS spectra of TAMRA−DNA-coated 15 nm AuNPs arranged on DNA origami substrates (red) and DNA origami structures modified with a single TAMRA molecule placed in the hot spot between two 25 nm AuNPs (the black spectrum is an average of several spots, and the blue spectrum was obtained from a single spot). In the blue and black SERS spectra, the TAMRA signal at 1647 cm^{-1} is still detectable. The other signals at 1589, 1275, and 1093 cm^{-1} are ascribed to the DNA surrounding the AuNPs, whereas the weak band at 1451 cm^{-1} is due to the Si/SiO_2 substrate. (c) AFM image of the same spot from which the blue SERS spectrum was obtained. Accordingly, a maximum of 17 isolated TAMRA molecules contribute to the Raman signal in the blue spectrum. On the right, the height profile of a AuNP dimer indicated by a blue line in the AFM image is shown.

EXPERIMENTAL METHODS

Triangular DNA origami were synthesized as previously described[27] from the M13mp18 viral scaffold (New England Biolabs) using the original design by Rothemund.[10] For the binding of the AuNPs, three staple strands per AuNP (t-6s27f, t-5s26e, t-4s27f, and t-1s6i, t1s6i, t1s8i in Rothemund's original notation) were extended on their 5′-end by the capture

dx.doi.org/10.1021/jz402076b | J. Phys. Chem. Lett. 2013, 4, 4140−4145

sequence 5′-$(AAT)_8T_4$-3′. For the introduction of the three TAMRA molecules, three staple strands located between the capture sites (t-3s6e, t-2s7f, and t-1s6e) were modified to carry a 5′ TAMRA modification. For the DNA origami with only one TAMRA modification, only the modified staple strand t-1s6e was used. All staple strands were purchased from Metabion.

DNA-coated AuNPs were prepared similar to the protocol of Ding et al.[12] Phosphinated AuNPs were coated with DNA in 0.5 × TAE with 50 mM NaCl (both from Sigma Aldrich) by adding a 200-fold excess of 3′ disulfide-modified oligonucleotides of the sequence 5′-$(ATT)_3T_4$-3′ (for 5 nm AuNPs) or 5′-$(ATT)_8T_4$-3′ (for 15 nm AuNPs) (Metabion). The resulting solution was left at room temperature for at least 80 h. Unbound oligos were removed by spin filtering the AuNP solution (50 μL + 200 μL of 1 × TAE with 10 mM $MgCl_2$, Sigma Aldrich) using Amicon Ultra-0.5 filters (100 kDa MWCO, Millipore) for 10 min at 2400 g, followed by washing with 300 μL of 1 × TAE-$MgCl_2$. For TAMRA-modified 15 nm AuNPs, oligonucleotides of the sequence 5′-$(ATT)_8T_3$X-SS-3′, with X = TAMRA, have been used (Metabion).

A 2 μL aliquot of the DNA origami sample (concentration ≈ 20 nM) was incubated for 1 h in 48 μL of 10 × TAE with 200 mM $MgCl_2$ on epi-polished Si(100) substrates with native oxide (1 × 1 cm^2, cleaned in an O_2 plasma). The substrates were then washed with 10−15 mL of 1:1 H_2O/ethanol and dried in a stream of N_2.

For hybridization of the adsorbed DNA origami with 5 nm AuNPs, 20 μL of the AuNP solution (50−100 nM) was then deposited on the substrate and incubated for 20 min at 21 °C. Excess AuNPs were removed by dipping the substrate for 10 s into Milli-Q water followed by drying in a stream of N_2.

The hybridization of DNA-modified 15 nm AuNPs to the DNA origami structures was performed in solution by incubation of an equimolar mixture (concentration of AuNPs and DNA origami ≈ 50 nM) for 7 h at 30 °C. Subsequently, the DNA origami structures were deposited on Si(100) substrates, as described above. The DNA-modified 15 nm AuNPs without a DNA origami substrate were deposited on Si(100) in the same way.

Electroless deposition was performed at 21 °C using GoldEnhance LM/Blot from Nanoprobes. The four solutions were mixed as suggested by the manufacturer and diluted 1:1 in 1 × TAE-$MgCl_2$ buffer before applying 20 μL of the resulting solution to the Si substrates with the adsorbed AuNP-decorated DNA origami. The deposition time was varied between 30 and 100 s before washing the sample with 1 mL of Milli-Q water. The size of the AuNPs was determined as a function of deposition time from AFM images, and a constant growth rate of 2.5 Å/s was obtained (see Figure S5, Supporting Information). AFM imaging was performed in air using a Bruker MultiMode 8 (Figures 1, 4, S1, and S5 (Supporting Information)) and a Nanosurf FlexAFM (Figures 2 and S2 (Supporting Information)) scanning probe microscope operated in tapping mode.

SERS spectra have been recorded using a confocal Raman microscope (WITec 300α) equipped with an upright optical microscope. For Raman excitation, laser light at 532 nm was used that was coupled into a single-mode optical fiber and focused through a 100× objective (Olympus MPlanFL N, NA = 0.9) to a diffraction-limited spot of about 1.3 μm^2. The laser power was set between 0.4 and 1 mW, and the integration time was either 2 s (for TAMRA coated AuNPs, Figure 2) or 10 s (for TAMRA bound to DNA origami structures; Figures 3 and 4). The coverage of DNA origami structures was chosen such that about 10 DNA origami structures were located in the laser focus area. The Raman spectra presented in Figures 2 (red) and 4 (red and black) are averages from different spots. The other displayed Raman spectra were collected from a single spot and correlated with AFM images using the following procedure: (i) introduction of a macroscopic marker, namely, a scratch in the Si samples, (ii) scanning of approximately the same 15 × 15 μm^2 area close to the marker by AFM (1024 × 1024 pixels) and confocal Raman microscopy (30 × 30 pixels), (iii) identification of pronounced surface features in both images that allow for an overlay of the images, and (iv) assignment of individual Raman spectra to surface topography recorded by AFM.

■ ASSOCIATED CONTENT

Ⓢ Supporting Information

Extended methods, characterization of DNA origami−AuNP hybrids by AFM (Figure S1), AFM image and Raman spectra of AuNPs covered with TAMRA-modified DNA (Figures S2 and S3), SERS spectra on different substrates (Figure S4), AuNP growth rate (Figure S5), simulated absorbance spectra (Figure S6), comparison of SERS intensity and electric field intensity (Figure S7), and SERS spectrum of the control sample (Figure S8). This material is available free of charge via the Internet at http://pubs.acs.org.

■ AUTHOR INFORMATION

Corresponding Authors

*E-mail: a.keller@hzdr.de.
*E-mail: bald@uni-potsdam.de.

Notes

The authors declare no competing financial interest.

■ ACKNOWLEDGMENTS

We thank S. Benemann and Dr. R. Bienert at the BAM for recording SEM images and S. Facsko for discussions. This research was supported by a Marie Curie FP7 Integration Grant within the 7th European Union Framework Programme, by the Deutsche Forschungsgemeinschaft (DFG), the University of Potsdam, and the Alexander von Humboldt Foundation.

■ REFERENCES

(1) Willets, K. A.; Van Duyne, R. P. Localized Surface Plasmon Resonance Spectroscopy and Sensing. *Annu. Rev. Phys. Chem.* **2007**, *58*, 267−297.

(2) Kneipp, K.; Wang, Y.; Kneipp, H.; Perelman, L. T.; Itzkan, I.; Dasari, R.; Feld, M. S. Single Molecule Detection Using Surface-Enhanced Raman Scattering (SERS). *Phys. Rev. Lett.* **1997**, *78*, 1667−1670.

(3) Kneipp, J.; Kneipp, H.; Kneipp, K. SERS — A Single-Molecule and Nanoscale Tool for Bioanalytics. *Chem. Soc. Rev.* **2008**, *37*, 1052−1060.

(4) Le Ru, E. C.; Etchegoin, P. G. Single-Molecule Surface-Enhanced Raman Spectroscopy. *Annu. Rev. Phys. Chem.* **2012**, *63*, 65−87.

(5) Lee, H. M.; Jin, S. M.; Kim, H. M.; Suh, Y. D. Single-Molecule Surface-Enhanced Raman Spectroscopy: A Perspective on the Current Status. *Phys. Chem. Chem. Phys.* **2013**, *14*, 5276−5287.

(6) Cao, Y. W. C.; Jin, R. C.; Mirkin, C. A. Nanoparticles with Raman Spectroscopic Fingerprints for DNA and RNA Detection. *Science* **2002**, *297*, 1536−1540.

(7) Graham, D.; Thompson, D. G.; Smith, W. E.; Faulds, K. Control of Enhanced Raman Scattering Using a DNA-Based Assembly Process of Dye-Coded Nanoparticles. *Nat. Nanotechnol.* **2008**, *3*, 548−551.

(8) Lim, D.-K.; Jeon, K.-S.; Hwang, J.-H.; Kim, H.; Kwon, S.; Suh, Y. D.; Nam, J.-M. Highly Uniform and Reproducible Surface-Enhanced Raman Scattering from DNA-Tailorable Nanoparticles with 1-nm Interior Gap. *Nat. Nanotechnol.* **2011**, *6*, 452−460.
(9) Lim, D.-K.; Jeon, K.-S.; Kim, H. M.; Nam, J.-M.; Suh, Y. D. Nanogap-Engineerable Raman-Active Nanodumbbells for Single-Molecule Detection. *Nat. Mater.* **2010**, *9*, 60−67.
(10) Rothemund, P. W. K. Folding DNA to Create Nanoscale Shapes and Patterns. *Nature* **2006**, *440*, 297−302.
(11) Pal, S.; Deng, Z. T.; Ding, B. Q.; Yan, H.; Liu, Y. DNA-Origami-Directed Self-Assembly of Discrete Silver-Nanoparticle Architectures. *Angew. Chem., Int. Ed.* **2010**, *49*, 2700−2704.
(12) Ding, B. Q.; Deng, Z. T.; Yan, H.; Cabrini, S.; Zuckermann, R. N.; Bokor, J. Gold Nanoparticle Self-Similar Chain Structure Organized by DNA Origami. *J. Am. Chem. Soc.* **2010**, *132*, 3248.
(13) Kuzyk, A.; Schreiber, R.; Fan, Z. Y.; Pardatscher, G.; Roller, E. M.; Hogele, A.; Simmel, F. C.; Govorov, A. O.; Liedl, T. DNA-Based Self-Assembly of Chiral Plasmonic Nanostructures with Tailored Optical Response. *Nature* **2012**, *483*, 311−314.
(14) Acuna, G. P.; Moller, F. M.; Holzmeister, P.; Beater, S.; Lalkens, B.; Tinnefeld, P. Fluorescence Enhancement at Docking Sites of DNA-Directed Self-Assembled Nanoantennas. *Science* **2012**, *338*, 506−510.
(15) Pal, S.; Dutta, P.; Wang, H. N.; Deng, Z. T.; Zou, S. L.; Yan, H.; Liu, Y. Quantum Efficiency Modification of Organic Fluorophores Using Gold Nanoparticles on DNA Origami Scaffolds. *J. Phys. Chem. C* **2013**, *117*, 12735−12744.
(16) Joseph, V.; Matschulat, A.; Polte, J.; Rolf, S.; Emmerling, F.; Kneipp, J. SERS Enhancement of Gold Nanospheres of Defined Size. *J. Raman Spectrosc.* **2011**, *42*, 1736−1742.
(17) Park, T.; Lee, S.; Seong, G. H.; Choo, J.; Lee, E. K.; Kim, Y. S.; Ji, W. H.; Hwang, S. Y.; Gweon, D. G. Highly Sensitive Signal Detection of Duplex Dye-Labelled DNA Oligonucleotides in a Pdms Microfluidic Chip: Confocal Surface-Enhanced Raman Spectroscopic Study. *Lab Chip* **2005**, *5*, 437−442.
(18) Stokes, R. J.; Macaskill, A.; Lundahl, P. J.; Smith, W. E.; Faulds, K.; Graham, D. Quantitative Enhanced Raman Scattering of Labeled DNA from Gold and Silver Nanoparticles. *Small* **2007**, *3*, 1593−1601.
(19) Mock, J. J.; Hill, R. T.; Degiron, A.; Zauscher, S.; Chilkoti, A.; Smith, D. R. Distance-Dependent Plasmon Resonant Coupling between a Gold Nanoparticle and Gold Film. *Nano Lett.* **2008**, *8*, 2245−2252.
(20) Cutler, J. I.; Auyeung, E.; Mirkin, C. A. Spherical Nucleic Acids. *J. Am. Chem. Soc.* **2012**, *134*, 1376−1391.
(21) Draine, B. T.; Flatau, P. J. Discrete-Dipole Approximation for Scattering Calculations. *J. Opt. Soc. Am. A* **1994**, *11*, 1491−1499.
(22) Flatau, P. J.; Draine, B. T. Fast Near Field Calculations in the Discrete Dipole Approximation for Regular Rectilinear Grids. *Opt. Express* **2012**, *20*, 1247−1252.
(23) Jang, N. H. The Coordination Chemistry of DNA Nucleosides on Gold Nanoparticles as a Probe by SERS. *Bull. Korean Chem. Soc.* **2002**, *23*, 1790−1800.
(24) Treffer, R.; Lin, X.; Bailo, E.; Deckert-Gaudig, T.; Deckert, V. Distinction of Nucleobases — A Tip-Enhanced Raman Approach. *Beilstein J. Nanotechnol.* **2011**, *2*, 628−637.
(25) Wustholz, K. L.; Henry, A. I.; McMahon, J. M.; Freeman, R. G.; Valley, N.; Piotti, M. E.; Natan, M. J.; Schatz, G. C.; Van Duyne, R. P. Structure−Activity Relationships in Gold Nanoparticle Dimers and Trimers for Surface-Enhanced Raman Spectroscopy. *J. Am. Chem. Soc.* **2010**, *132*, 10903−10910.
(26) Rinker, S.; Ke, Y.; Liu, Y.; Chhabra, R.; Yan, H. Self-Assembled DNA Nanostructures for Distance-Dependent Multivalent Ligand−Protein Binding. *Nat. Nanotechnol.* **2008**, *3*, 418−422.
(27) Keller, A.; Bald, I.; Rotaru, A.; Cauet, E.; Gothelf, K. V.; Besenbacher, F. Probing Electron-Induced Bond Cleavage at the Single-Molecule Level Using DNA Origami Templates. *ACS Nano* **2012**, *6*, 4392−4399.